Astron. Astrophys. 54, 703—711 (1977)

ASTRONOMY AND ASTROPHYSICS

High Resolution Observations of M 51 at 21 and 49 cm

A. Segalovitz

Sterrewacht, Huygens lab., Wassenaarseweg 78, Leiden 2405, The Netherlands

Received July 19, 1976

Summary. Recent observations of M 51 at 21 cm and at 49 cm done with the Westerbork Synthesis Radio Telescope are presented. The spectral index, α_{21-49}, is determined for a large part of the galaxy and it is found to be characteristically 0.65 in the nuclear region, 0.7 across the disk and 0.8 in the outer parts.

The continuum radiation has about the same extent as the optical radiation on very long exposure photographs and the *21 cm line* radiation. Some features which are detected in the faint outer structure are suggestive of a continuation of a spiral arm.

Peaks along the arms are found to be $\sim$1.3 kpc apart and roughly symmetrically located with respect to the nucleus. The arms/disk contrast is determined to be typically 1.7.

Key words: M 51 — spiral galaxies: radio emission from — spiral galaxies: radio spectral index distribution of

1. Introduction

Single dish and aperture synthesis observations of Messier 51 have been carried out by many observers [see list in Segalovitz (1976a)]. We have chosen to observe the galaxy at 49 cm in order to explore the outer regions of the galaxy. The Westerbork Synthesis Radio Telescope (WSRT) provides at this wavelength a resolution lower than that of previous observations of M 51 at 21 and 6 cm. However, due to the non-thermal nature of the radio radiation coming from M 51, the signal at 49 cm is about 2 times stronger than that at 21 cm which gives observations at 49 cm an advantage. Also, the WSRT system temperature for 21 cm has been reduced by about a factor of 2.5 since the previous observations of Mathewson, van der Kruit and Brouw (1972) and we have, therefore, reobserved the galaxy at 21 cm. This enables us to get the spectral index, α_{21-49} ($S \propto \nu^{-\alpha}$), over a large part of the galaxy and to detect emission farther from the center than was previously possible. The signal to noise ratio of the new 21 cm observations enables us to delete a considerable number of the shorter spacings while still retaining most of the intense peaks well above the noise. We could, therefore, produce high resolution maps of the small scale structures within the galaxy. More details concerning this procedure are given in Section 3.2.3.

2. Observations

A description of the observations is given in Table 1. A detailed description of the instrument can be found elsewhere (Baars and Hooghoudt, 1974; Högbom and Brouw, 1974; Casse and Muller, 1974; van Someren Gréve, 1974).

Five intensity maps were produced, all of which were reduced using the "clean" procedure (Högbom, 1974; Harten, 1974, 1976). These maps are denoted M_1 through M_5 and are described in Table 1. All of them were corrected for the primary beam attenuation. Map M_1 was prepared from all the baselines available at $\lambda = 49$ cm. In order to compare the 21 cm observations with the 49 cm observations, baselines shorter than 183 wavelengths (90 m) were deleted from the 49 cm set of baselines (map M_2) while baselines longer than 2887 wavelengths (612 m) were deleted from the 21 cm set of baselines (map M_5). Both maps were cleaned and restored with the same beam. Two additional maps were produced from the 21 cm set of interferometers. A map composed of all the baselines available (M_3) and a map composed of baselines longer than 2887 wavelengths (612 m) and shorter than 6877 wavelengths (1458 m). In the latter, which is denoted M_4, features larger than 1′ are resolved. At the same time, the resultant antenna pattern has a half power width narrower than that of M_3 and a first side lobe at a level of about -30%.

All the results concerning polarization together with a discussion are presented elsewhere (Segalovitz et al., 1976) where they are compared with polarization detection in M 81 and in M 31.

Table 1. Observational and instrumental parameters

Map code	M_1	M_2	M_3	M_4	M_5
Frequency; Bandwidth (MHz; MHz)	610; 4.0	←	1415; 4.0	←	←
HPW of synthesized and of restoring beam (RA″ × DEC″)	56 × 76	←	24 × 32	19 × 25	56 × 76
1 K is equivalent to ... (mJy/beam)	1.5	←	←	0.9	8.2
R.M.S. noise (mJy/beam; K)	0.65; 0.42	←	0.25; 0.17	0.32; 0.35	0.4; 0.048
Observing dates (day/month/year)	23,31/1/75	←	7,21/6/75	←	←
	2,28/2/75	←	5/7/75	←	←
	3,19/3/75	←	7/8/75	←	←
Observing time (hours)	4 × 12	←	←	←	←
Baseline coverage from, to, by (meters)	36, 1458, 18	90, 1458, 18	36, 1458, 18	630, 1458, 18	36, 612, 18
Primary beam, HPW (arcmin)	83	←	36	←	←
Shortest baseline corresponds to features on a scale of ... (arcmin)	47	18.8	20.2	1.16	20.2
Number of figure in this paper	–	1	3	4	2

3. Reduction and Results

3.1. *Observations at* $\lambda = 49$ cm

3.1.1. The Cleaning Process and the Integrated Flux. The spacings related to M_2 (Table 1) were combined to produce an intensity map. The map has been cleaned down to components at a level of 1 σ (0.65 mJy/beam) and restored with a gaussian beam which had the same half power width (HPW) as the synthesized beam: 56″ × 76″. The sum of the clean components is 2650 mJy. There may be another 100 mJy below the clean limit scattered all over the galaxy. This is estimated from the map of the remains after cleaning all the components above 1 σ. We therefore estimate the integrated flux to be 2750 mJy.

To compare our figure for the integrated flux density, S_{610}, with single dish measurements we have linearly interpolated on a log – log scale between the figures given by (a) Caswell and Wills (1967) at 178 MHz and each of the two: (b) Heeschen and Wade (1964) at 750 MHz and (c) Kuril'chik (1966) at 920 MHz. The interpolation between (a) and (b) gives $S_{610} = 2680$ mJy while the interpolation between (a) and (c) gives $S_{610} = 2800$ mJy. Both of these are in good agreement with our figure.

3.1.2. Comparison of M_1 *and* M_2. The 49 cm map of M 51 which was made from all the available spacings, M_1, is not shown in this paper. The reason is that its contours are identical in shape and intensity to those of the map prepared without the inclusion of the shorter spacings (M_2, Fig. 1). This is due to the fact that the size of the part of the galaxy which is above the noise is considerably smaller than the size of the largest feature detectable in M_2 (see Table 1).

3.1.3. The Structure of M 51 *at* 49 cm. Very few details can be observed in the inner parts of the galaxy with a beam size of ~1′. The outer parts, however, are detected for the first time with such a resolution. Figure 1 shows that the galaxy has a low level large scale radio component which extends further out than the optical boundaries on our photographs. The size of the radio picture is comparable with the optical size on very long exposure photographs of M 51 e.g. the one taken by Burkhead and Kalinowski (1975) or the one taken by H. Arp (private communication). The radio extension all along the eastern side of the galaxy corresponds to elongated optical features which extend from the northern and southern parts of the galaxy.

3.2. *The Different Maps at* 21 cm

3.2.1. The Convolved $\lambda = 21$ cm *Map* (M_5). The 21 cm map M_5 (Fig. 2) was made from spacings which were chosen so that the resultant beam would be as similar as possible to the 49 cm beam of M_2. The map was then cleaned down to a level of 1 σ (0.4 mJy/beam) and restored with a gaussian beam identical to the one used for M_2.

The sum of the clean components is 1480 mJy with possibly another 50 mJy under the clean limit. This is in good agreement with the single dish measurements of de Jong (1966): $S_{21.2} = 1600 \pm 80$ mJy and of Lequeux (1971): $S_{21.1} = 1510 \pm 120$ m.f.u.

Five sources are marked by arrows in Figure 2. They are designated 1 through 5. Probably four of them are external sources unassociated with the galaxy while source 3 may be a supernova remnant (Mathewson et al., 1972). Some of these sources are discussed later on.

3.2.2. The $\lambda = 21$ cm *Full Resolution Map* (M_3). The map M_3 was prepared using all the spacings available at 21 cm (Fig. 3). With a beam of 24″ × 32″ it is comparable in resolution to previous WSRT observations of M 51 at 21 cm (Mathewson et al., 1972) but has a considerably lower noise. Note that the outer eastern part of the galaxy shows some structure on a level somewhat higher than 2 σ. This is significant because these same regions are also observed at a level of 3 σ or more both at 21 cm (M_5, Fig. 2) and at 49 cm, Fig. 1). The shape of this low level structure is suggestive of a continuation for half a

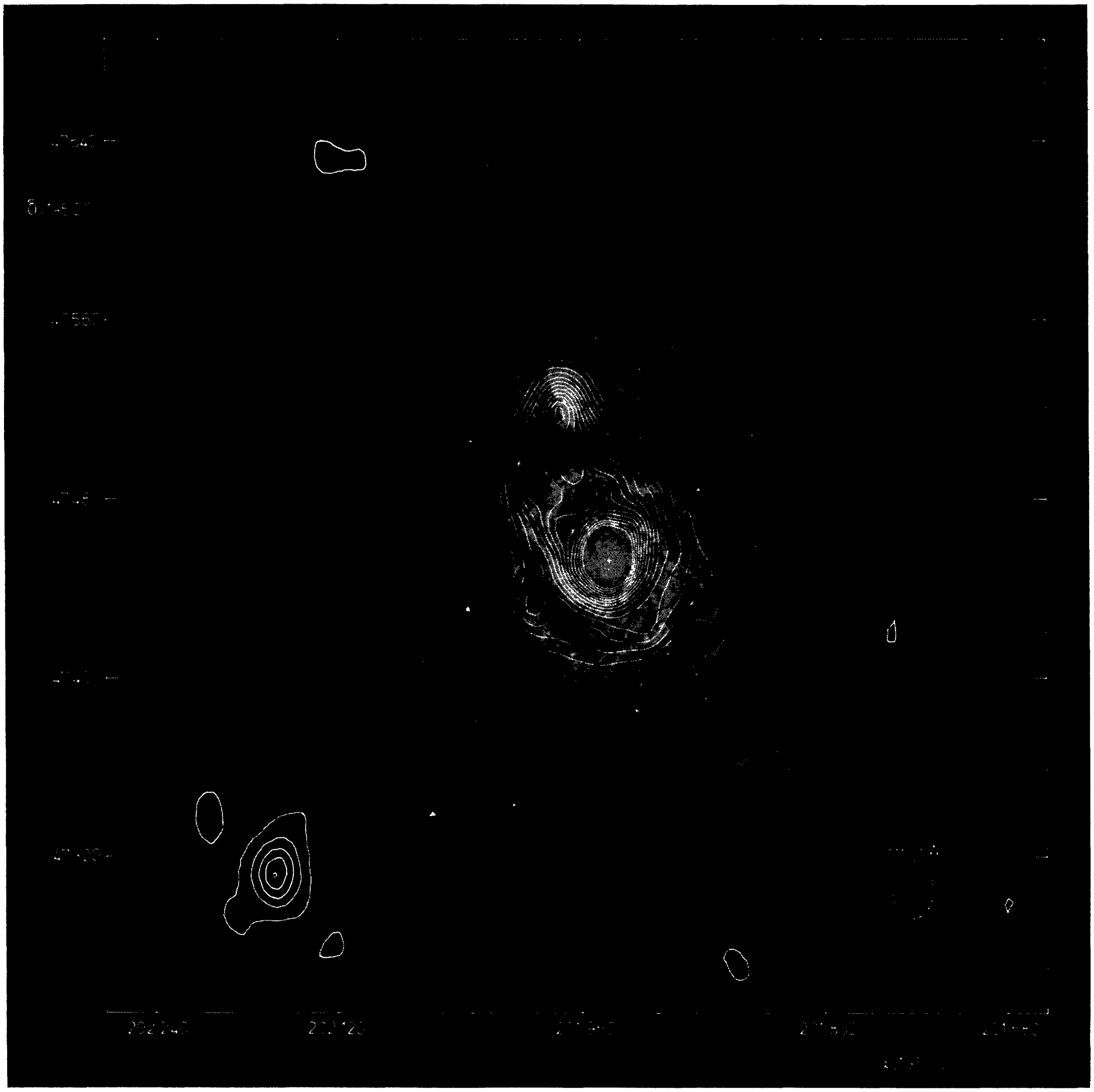

Fig. 1. Contour map of the radio brightness of M 51 at 49 cm superposed on a blue photograph of the galaxy. Four reference stars, the optical center and the field center (~1.2′ NE of the nucleus) are marked by crosses. Contour levels are from 2 to 172 every 10 mJy/beam (in K: 1.3 to 112 every 6.5). This map is designated M_2 and is produced from spacings ranging from 90 to 1458 every 18 m (see Table 1). The noise level is 0.65 mJy/beam

revolution of the spiral arm which otherwise seems to end at the southern part of M 51. Most of the peaks of this low level structure appear coincident with the faint elongated optical features mentioned in Section 3.1.3. A possible continuation of the outermost southwest spiral arm *in the* 21 cm *line* was first observed and discussed by Weliachew and Gottesman (1973).

3.2.3. The $\lambda = 21$ cm "*Narrow Beam*" *Map* (M_4). The map M_4 was made from spacings larger than 612 m. Deleting the shorter spacings has the following effects on the resultant antenna pattern: First, the beam ($\text{HPBW}_\alpha \times \text{HPBW}_\delta = 19'' \times 25'' = 0.9 \times 1.17$ kpc) is smaller than that of M_3. Second, the first side lobe is on a level of -30% compared to -5% of the beam of M_3. Third, features on a scale larger than 1′ are resolved. Figure 4 shows the cleaned and restored map. This is the highest resolution map so far obtained at radio wavelengths which shows such a large part of the spiral structure of M 51. Mathewson et al. (1972, p. 478) already noted that the two spiral arms coming from the nucleus have a remarkable similarity of the variations of intensity *along the spiral arms* on a scale of ~30″. They state that the similarity holds up to a distance of ~0.06° *along the arms* starting from their origin near

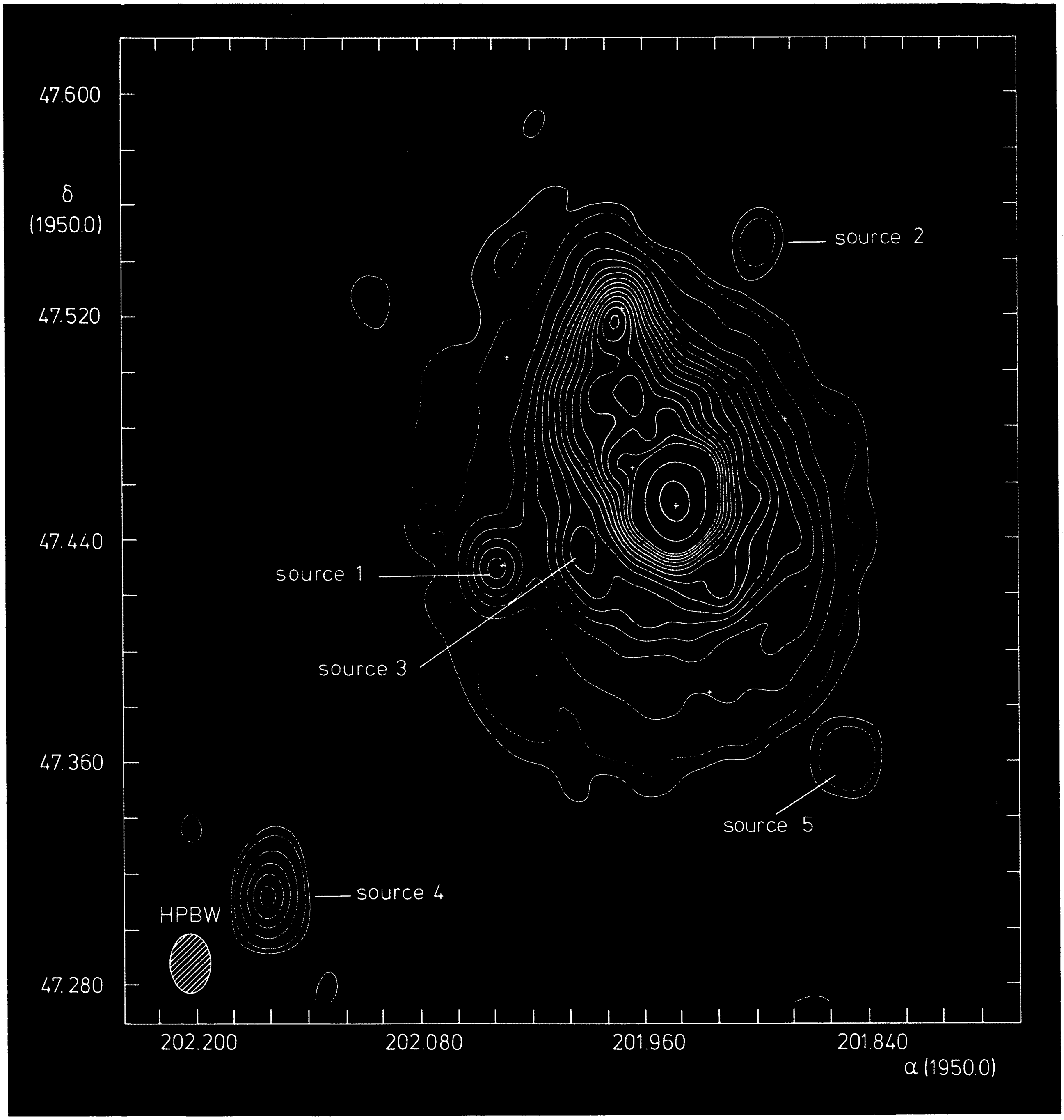

Fig. 2. A convolved map of M 51 at 21 cm. The HPBW is 56″ × 76″. Contour levels are from 1.2 to 71.2 every 5 mJy/beam and two additional contours at 2.4 and 100 mJy/beam (in K: from 0.14 to 8.6 every 0.6, 0.3 and 12). This map is designated M_5 in Table 1 and is produced from spacings ranging from 36 m to 612 m every 18 m. The noise level is 0.4 mJy/beam. The optical center of the galaxy, the field center and four reference stars are marked by crosses

the nucleus. We detect about twice as many peaks as they do and confirm this similarity on a resolution scale smaller by ~20%. Most of the peaks in one arm have corresponding peaks on the other arm such that the pairs are roughly symmetrically located with respect to the nucleus. We find that this similarity extends up to a distance of ~22 kpc (0.13°) *along the arms* and that a typical distance between the peaks is 0.008° (1.3 kpc at a distance of 9.7 Mpc) in the plane of the galaxy. Only the WSRT 6 cm observations (Segalovitz, 1976a) provide a higher resolution picture of the spiral structure of M 51 at radio wavelengths (though severely limited in signal to noise ratio). The 15″ × 15″ resolution map of M 51 at 6 cm does not change the above figure of 0.008°. The full resolution 6 cm map, with a much smaller beam of 6.8″ × 9.2″, shows a somewhat higher density of peaks

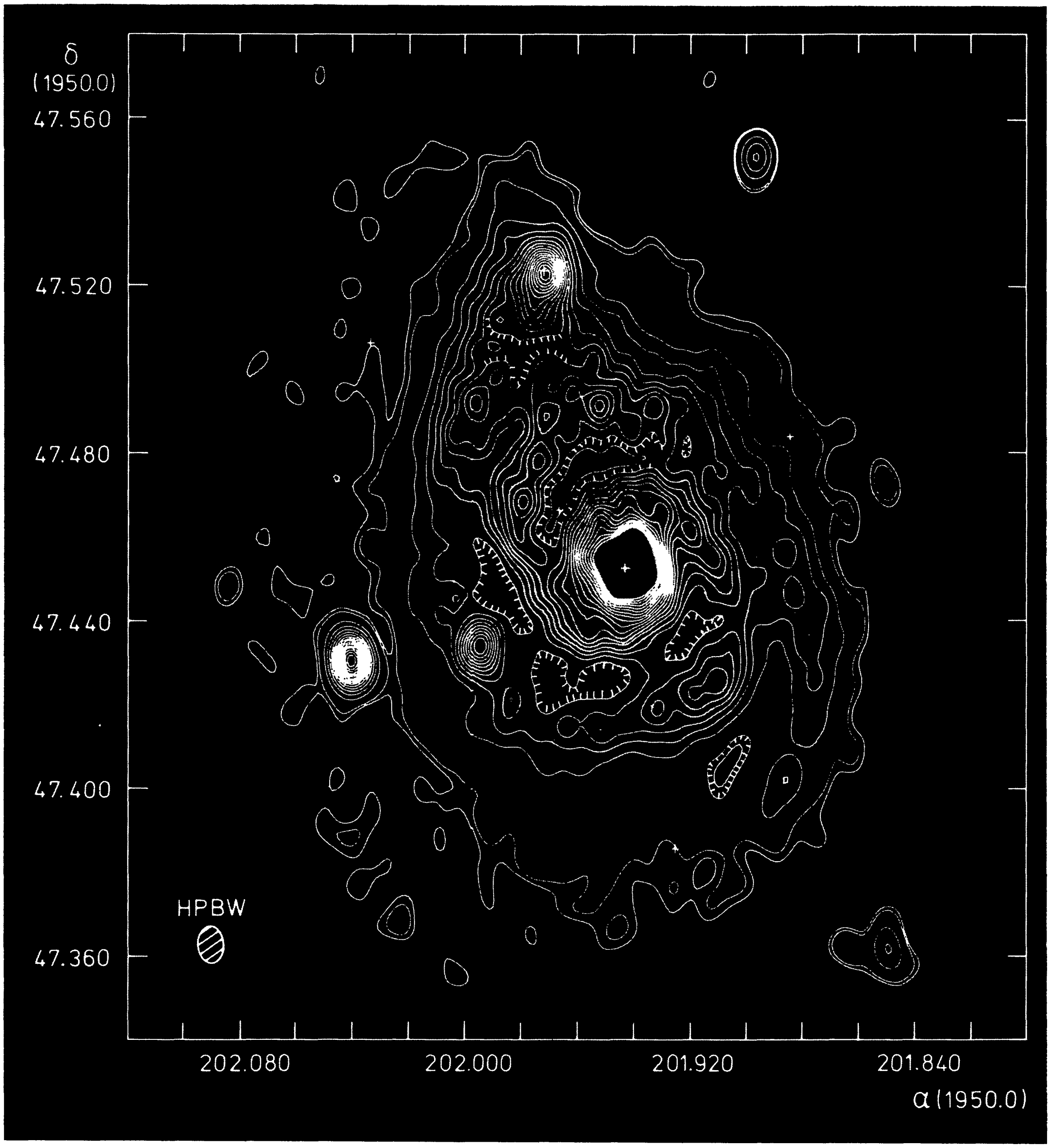

Fig. 3. The full resolution map at 21 cm prepared from spacings ranging from 36 m to 1458 m every 18 m. Contour levels are from 0.75 to 29.25 every 1.5 mJy/beam and an additional contour at 0.5 mJy/beam (in K: from 0.5 to 19.6 every 1 and 0.33). This map is designated M_3 in Table 1. The noise level is 0.25 mJy/beam (0.17 K)

along the arms (typical separation $\sim$800 pc) in the inner regions (galactocentric distance <2.5 kpc$=0.015°$). In Figure 5 we have plotted the peaks we detect at 6 cm in the $15'' \times 15''$ resolution map (for $r \geqq 2.5$ kpc) and in the $6.8'' \times 9.2''$ map (for $r<2.5$ kpc) which are within the first contour of Figure 4. Although the typical separation is close to the resolution limit, we find that, considering the confirmation by the 6 cm results, our figure is meaningful.

Since features on a scale larger than 1′ are strongly attenuated in M_4, we may take the intensities in Figure 4 to represent the *difference* between intensity peaks and the general disk emission. We find that a characteristic peak in the arm has $T_{b,\,21.2}=4$ K *above* a general disk emission characteristically of $T_{b,\,21.2}=6$ K. This is true for radii smaller than 7 kpc ($\sim$0.04°). Note that a correction to face on values may change these numbers by $\sim$20% but not the ratio.

3.3. *Comparison of the* 49 cm *and the* 21 cm *Results*

We should stress here, before we go into the comparison itself, a few points which are important for the derivation of the spectral index distribution further in this section. The "clean" method, which has been applied to both the 21 and the 49 cm maps, removes not only the near-in side

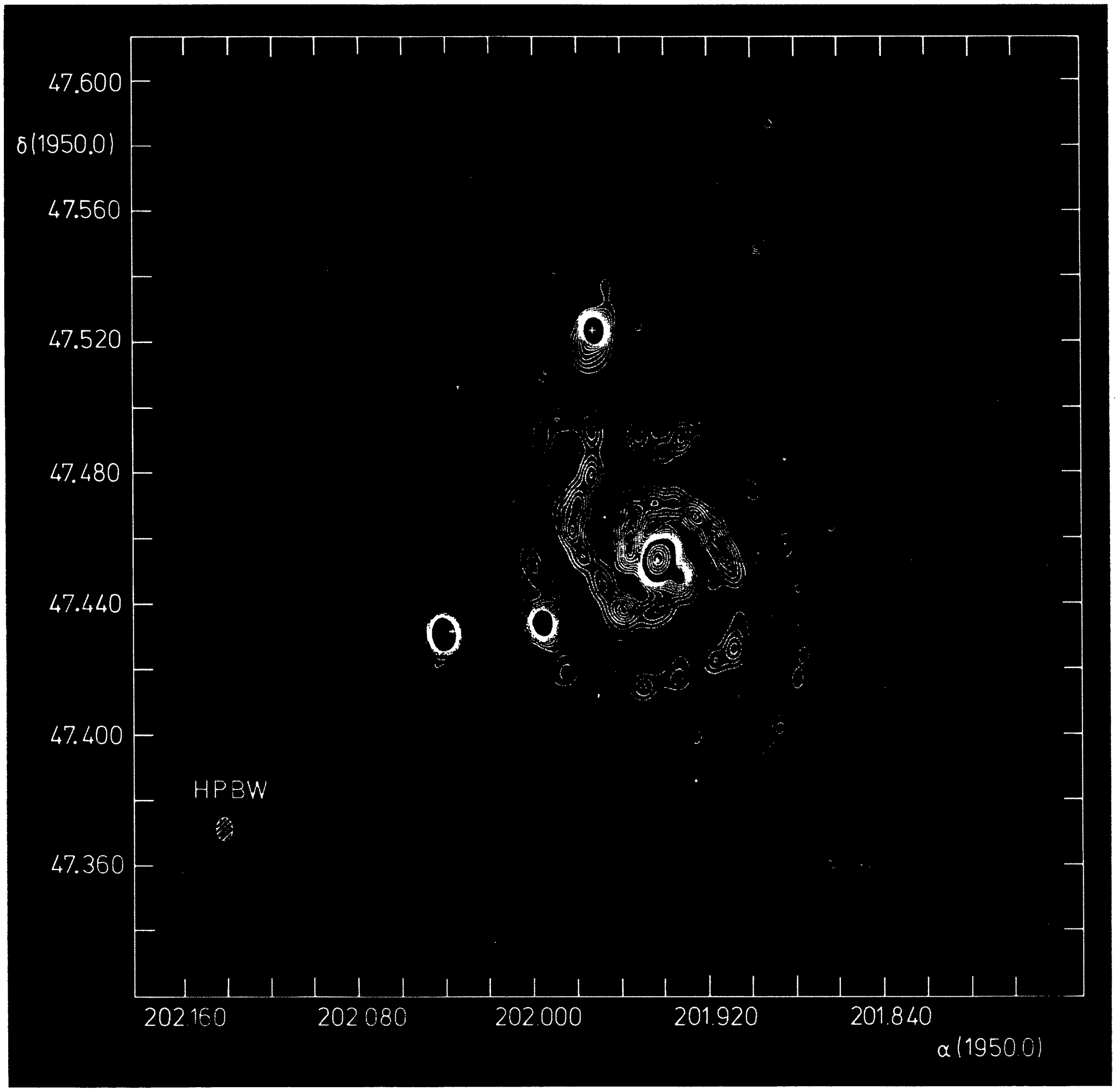

Fig. 4. A high resolution map of M 51 at 21 cm. This map is designated M_4 in Table 1 and is made from spacings ranging from 630 to 1458 every 18 m. Features on a scale larger than 1′ are strongly attenuated in this map. Contour levels are from 0.85 to 6.85 every 0.75 mJy/beam and from 17 to 37 every 5 mJy/beam (in K: from 0.9 to 7.6 every 0.8 and from 19 to 41 every 5.5). The noise level is 0.32 mJy/beam (0.35 K)

lobes but also the large scale depression which is present in the synthesized beam due to the missing short spacings. The method, then, may be thought of as interpolating in the *u–v* plane into spatial features larger than those observed by the smallest-spacing interferometer. If the "clean" iterations are successful, then one may expect to find only noise at regions free of radiation. (The systematic tendency for negative values should disappear. See e.g. Rogstad and Shostak, 1971.) No theoretical proof has so far been given for the convergence of the "clean" components to the right solution but, practically, the method works very well (Fomalont and Wright, 1974). For the specific case of M_2, we have two independent pieces of evidence to show that, indeed, the "clean" method reconstructs the real intensity distribution of M 51: 1. The map M_1, in which none of the flux of M 51 is likely to be missing (due to the large scale of features related to the shortest specing), is *identical* to the cleaned and restored map, M_2 (see Section 3.1.2). This strongly indicates that, for the intensity distribution of M 51, a map composed of spatial frequencies larger than 1/18.′8 contains enough information for the "clean" method to accurately add the missing low spatial frequencies. 2. The high resolution Effelsberg 100 m single dish observations of M 51 at 6.25 cm indicate the same boundary for the galaxy as in M_2 (Wielebinski, private communication).

Since the 21 cm intensity distribution of M 51 is rather similar to the 49 cm distribution, we may safely assume that in M_5, too, the "clean" method provides the correct intensity distribution.

The two maps, M_5 and M_2, are, then, directly comparable because (a) they have the same beam, (b) the sensitivity of the 21 cm observations is higher, *partly*

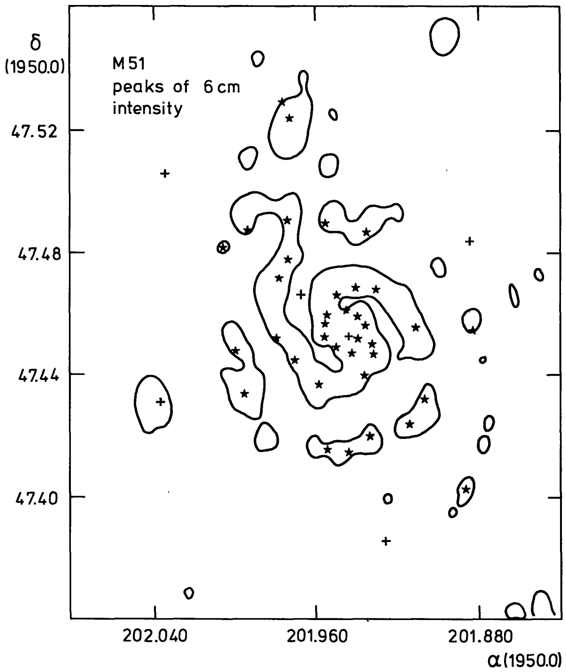

Fig. 5. Comparison of the location of peaks along the spiral arms at 6 cm and at 21 cm. The stars represent 6 cm peaks which were found *within* the first contour of Figure 4 which is redrawn here for easy reference. Four reference stars, the field center and the optical center of M 51 are marked by crosses

compensating for the non-thermal spectrum of the radiation and (c) they both contain practically all the flux which is measured by single dish measurements as coming from M 51 (see Sections 3.1.1 and 3.2.1). The outer contours in the two maps are roughly similar. This again suggests (see Section 3.1.2) that at the location of the lowest contour of the 49 cm map there occurs a sharp decrease in the 49 cm intensity. If this were not so then, keeping in mind the non-thermal spectrum of the radiation and the ratio of the sensitivities in M_2 and M_5, we should see the 49 cm radiation extending considerably further than the 21 cm radiation.

The maps M_5 and M_2 were used to derive the spectral index distribution defined by $\alpha_{21-49} = \ln(I(M_2)/I(M_5))/\ln(1415/610)$. The resultant map is shown in Figure 6. Only map grid points which were above a level of $10\,\sigma$ were used. The error *per grid point* varies from 0.15 for the outermost contours to 0.04 in the inner parts. This error estimate includes the uncertainty in the primary beam correction and the instabilities in the gain of the telescope receivers as given by Willis et al. (1976). This disk region is on a general level of $\alpha_{21-49} = 0.7$ with a general tendency of the spectrum to steepen towards the outer parts. To demonstrate this, we have chosen the following procedure: The average intensity was determined for *circles in the plane of the galaxy* at both 21 cm and 49 cm and the spectral index curve, α_{21-49}, was determined from these averages (Fig. 7). Only the R.M.S. noise of each of the maps, M_2 and M_5, contributes significantly to the errors. Other sources, like uncertainties in the primary beam attenuation and gain variation with time, are not significant due to the large number of independent beams per circle. A slightly different curve prepared from previous 21 cm observations of M 51 was presented by us elsewhere (Segalovitz, 1976b). The difference between the two curves, however, is not significant.

Source 4 (see Fig. 2) appears both on M_2 and on M_5. At 49 cm it has an extension which goes as far as 2.′3 north and south of the peak. We find on our higher resolution map (in the region of M_4 which is not included in Figure 4) that the central source is resolved into two components: a southern one which contains ~22 mJy and a northern one which contains ~3.5 mJy. Source 4 seems, therefore, to be an asymmetric double radio source with an extension roughly along its major axis (NS direction)

4. Summary and Discussion

For quick reference we summarize the main findings of this paper:

I. We find that (a) the lowest contours (~$3\,\sigma$ level) of the radio radiation from M 51 detected at 610 MHz (Figure 1, $3\,\sigma = 1.26$ K) and at 1415 MHz (Figure 2, $3\,\sigma = 0.14$ K) are located at roughly the same place. (This is *not* due to the large-scale-features attenuation of the WSRT. See Section 3.1.2.) The same boundary is found on the Effelsberg 100 m single dish map of M 51 at 6.25 cm. (b) These contours roughly correspond to the optical boundary of the galaxy on very long exposure photographs of M 51 [e.g. Burkhead and Kalinowski (1975), or photograph by Sydney van den Bergh *in* Toomre and Toomre (1973)].

II. On the eastern side of M 51 small scale elongated structures were detected which correspond to elongated optical features mentioned above and which are suggestive of a continuation of the spiral arm which seems to end south of the galaxy on the optical photograph used in this paper (Section 3.2.2).

III. A typical separation between intensity peaks along both spiral arms is found to be 0.008° (1.3 kpc at a distance of 9.7 Mpc) in the plane of the galaxy. The remarkable similarity of the variations of intensity *along the two spiral arms* found before (Mathewson et al., 1972) is confirmed on a resolution scale of ~22″. That similarity is found to extend to a distance of 22 kpc (0.13°) *along the arms* beginning at their origin near the nucleus. There are indications, based on 6 cm observations, that in the inner regions (galactocentric distance <2.5 kpc) the peaks may be somewhat closer to each other (separation of ~800 pc). Peaks in the arms are found to have $T_{b,\,21.2} = 4$ K *above* a general disk emission of $T_{b,\,21.2} = 6$ K for radii smaller than 7 kpc (~0.04°) (Section 3.2.3).

IV. The spectral index distribution of M 51, α_{21-49}, was determined (Fig. 6) and it was found that the nuclear

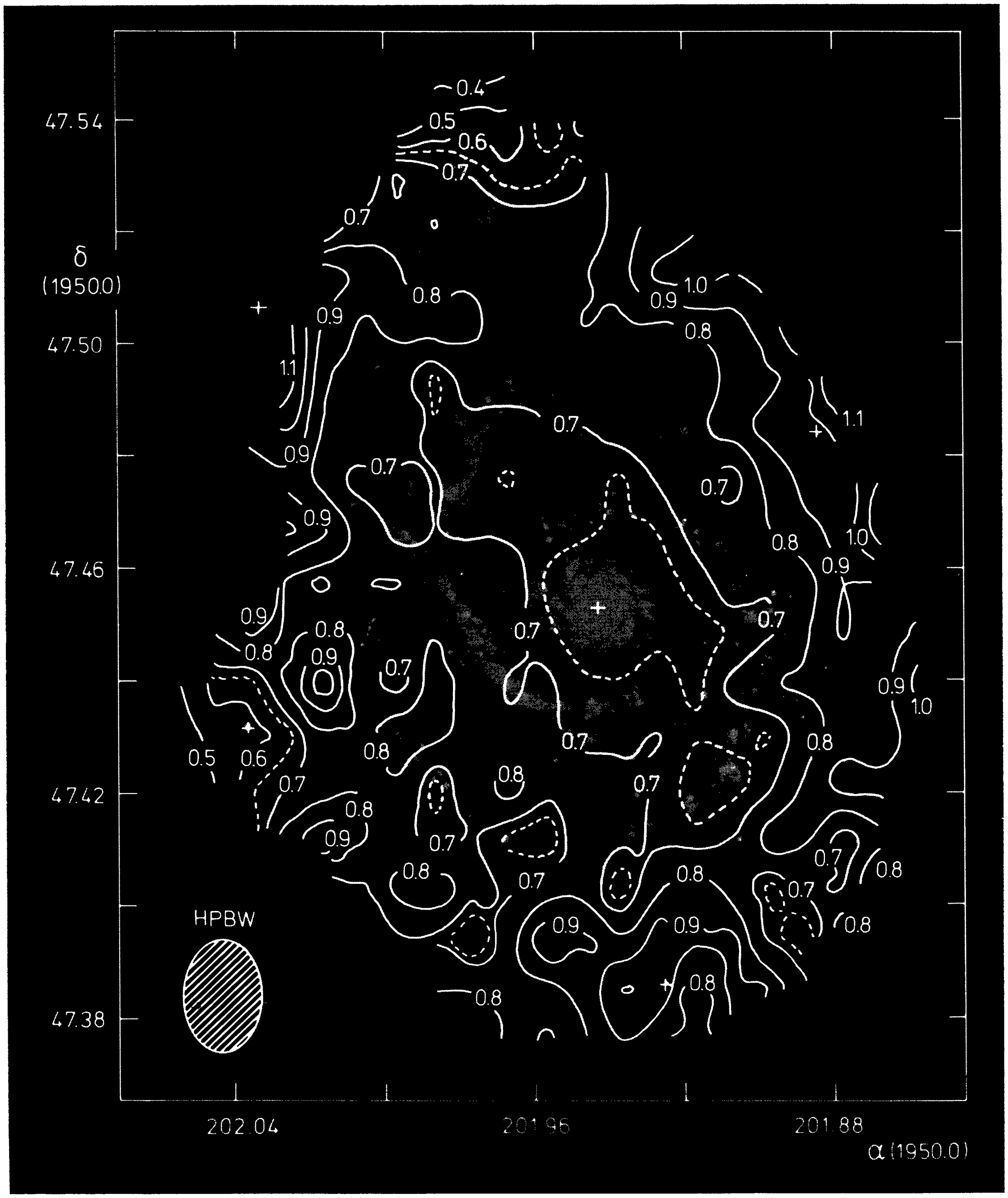

Fig. 6. The spectral index distribution, α_{21-49}, of M 51. Only grid points at a level higher than 10σ in the maps M_2 and M_5 (Figures 1 and 2 respectively) have been used. The spectral index is defined: $\alpha_{21-49} = \ln(F_{49}/F_{21})/\ln(49/21)$ where F_y denotes the flux density at $\lambda = y$ cm. The $\alpha = 0.65$ contour is drawn as a dashed line. In the outer parts the error in α is ~ 0.15 while in the inner parts it is ~ 0.04

region has $\alpha_{21-49} \simeq 0.65$, the disk has $\alpha_{21-49} \simeq 0.7$ and the outer parts have $\alpha_{21-49} \simeq 0.8$ (Fig. 7) (Section 3.3).

The author (Segalovitz, 1976b) has constructed models to explain point IV. One can show that the assumption of diffusion of relativistic electrons away from their birth places in a cyclindrically symmetrical system can explain the distribution of spectral index (Fig. 7) *and* the intensity distribution of M 51. Two sets of parameters produce models which fit the observations: (a) a constant magnetic field and diffusion coefficient with leakage of electrons out of the galactic magnetic field in the *z*-direction on a time scale of $\sim 10^7$ years, (b) no leakage but a magnetic field which is proportional to $1/r^{1/2}$ and a diffusion coefficient which is proportional to $1/r$ where r is the galactocentric distance.

From point *I* (part *a*) ist follows that either (1) the magnetic field of the galaxy has a well defined boundary or (2) the source of relativistic electrons is sharply cut off at the outer edge of the galaxy. In case (1) the weakening of the magnetic field is the reason for the weakening of the radio radiation in both wavelengths

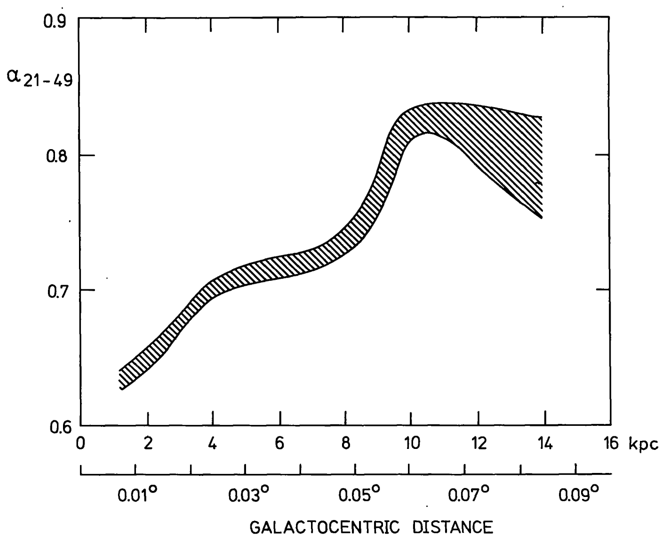

Fig. 7. The spectral index between 49 and 21 cm as determined from the average flux density along circles in the plane of the galaxy. The inclination was taken to be 35° and the position angle of the line of nodes was taken to be −14°. For every radius the range of α's is related to the range of intensities within 1 σ of the observed intensities

while in case (2) the sharp cut off in the source of electrons will cause strong streaming of electrons in the radial direction [see Figures 11 and 17 in Segalovitz (1976b)] which will result in a flattening of the spectrum at the location of the cut off. In that case the flatter spectrum will make us see the same boundary at 21 and 49 cm taking into consideration the noise ratio of the observations at the two wavelengths. If *neither* (1) *nor* (2) apply, then the diffusion of electrons in the radial direction would make the intensity structure appear to be more extended at $\lambda = 49$ cm than at $\lambda = 21$ cm because of the non-thermal spectrum of the radiation and given the σ levels in the 21 and 49 cm maps (see Table 1). At the same time, from part (b) of point *I*, we find that the optical and the continuum radio emission have about the same boundary as the 21 cm *line* emission (Shane and Bajaja, private communication; Shane, 1975; Weliachew and Gottesman, 1973) with the exception of a peculiar cloud south-east of the galaxy. It seems, therefore, that the lowest contour in Figure 1 or in Figure 2 is the edge of the galaxy as a whole.

The optical elongated features mentioned in Section 3.2.2 and in point II above were suggested (Toomre and Toomre, 1973) to be the result of the tidal interaction between M 51 and its companion. Inspection of the integrated H I map of M 51 (Shane and Bajaja, private communication) and of our map M_3 leads us to believe, however, that at least part of these elongated features is a natural continuation of the arm which seems, on our optical photographs, to end at the southern end of the galaxy.

Point III is consistent with the suggestion of Parker instabilities in the magnetic field on a scale of ~1 kpc (Mouschovias, 1974; Mouschovias et al., 1974; Shu, 1974; Mouschovias, 1975). However, we are not aware of a theory which could explain the symmetry of the intensity structure with respect to the nucleus. As for the intensity peaks, a characteristic value of 1.7 is suggested for the arms/disk contrast in accordance with the data quoted by Shane (1975). (The arms/disk contrast if defined as the peak intensity in the arm at a certain distance from the center divided by the general disk emission for the same radius. It is, therefore, equivalent to the peak-to-average contrast.)

Acknowledgements. I thank Prof. H. van der Laan, W. W. Shane and A. G. Willis for their critical reading of the manuscript. A grant from the Netherlands Organization for the Advancement of Pure Research (Z.W.O.) is acknowledged. The Westerbork Synthesis Radio Telescope is operated by the Netherlands Foundation for Radio Astronomy with the financial support of Z.W.O.

References

Baars, J. W. M., Hooghoudt, B. G.: 1974, *Astron. Astrophys.* **31**, 323
Burkhead, M. S., Kalinowski, J. K.: 1975, *Sky and Telescope* **50**, 95
Casse, J. L., Muller, C. A.: 1974, *Astron. Astrophys.* **31**, 333
Casswell, J. L., Wills, D.: 1967, *Monthly Notices Roy. Astron. Soc.* **135**, 231
Fomalont, B. F., Wright, M. C. H.: 1974, Galactic and Extra Galactic Radio Astronomy, Ed. G. L. Verschuur and K. I. Kellermann, Springer-Verlag, Berlin, p. 256
Harten, R. H.: 1974, Internal Technical Report No. 121, Netherlands Foundation for Radio Astronomy (SRZM), Dwingeloo
Harten, R. H.: 1976, in preparation
Heeschen, D. S., Wade, C. M.: 1964, *Astron. J.* **69**, 277
Högbom, J. A.: 1974, *Astron. & Astrophys. Suppl.* **15**, 417
Högbom, J. A., Brouw, W. N.: 1974, *Astron. Astrophys.* **33**, 289
Jong, M. L. de: 1966, *Astrophys. J.* **144**, 553
Kuril'chik, V. N.: 1966, *Soviet Astron.* **10**, 1
Lequeux, J.: 1971, *Astron. Astrophys.* **15**, 30
Mathewson, D. S., Kruit, P. C. van der, Brouw, W. N.: 1972, *Astron. Astrophys.* **17**, 468
Mouschovias, T. Ch.: 1974, *Astrophys. J.* **192**, 37
Mouschovias, T. Ch., Shu, F. H., Woodward, P. R.: 1974, *Astron. Astrophys.* **33**, 73
Mouschovias, T. Ch.: 1975, *Astron. Astrophys.* **40**, 191
Rogstad, D. H., Shostak, G. S.: 1971, *Astron. Astrophys.* **13**, 99
Segalovitz, A.: 1976a, *Astron. Astrophys.*, **52**, 167
Segalovitz, A.: 1976b, Ph. D. Thesis, Univ. of Leiden
Segalovitz, A., Shane, W. W., de Bruyn, A. G.: 1976, *Nature* **264**, 222
Shane, W. W.: 1975, High Resolution Observations of Neutral Hydrogen in M 51 *in the proceedings of the* Colloque International du CNRS sur «La Dynamique des Galaxies Spirales», ed. L. Weliachew, page 217
Shu, F. H.: 1974, *Astron. Astrophys.* **33**, 55
Someren Gréve, H. W. van: 1974, *Astron. Astrophys. Suppl.* **15**, 343
Toomre, A., Toomre, J.: 1973, *Sci. American* **229**, 38
Weliachew, L., Gottesman, S. T.: 1973, *Astron. Astrophys.* **24**, 59
Willis, A. G., Oosterbaan, C. E., Ruiter, H. R. de: 1976, *Astron. Astrophys. Suppl.*, in press